Automated Intersection Mapping from Crowd Trajectory Data

Christian Ruhhammer, Michael Baumann, Valentin Protschky, Horst Kloeden, Felix Klanner and Christoph Stiller, *Senior Member, IEEE*

***Index Terms*—Crowd Sourcing, Data Mining, Fleet Data, Traffic Light Detection.**

***Abstract*—Driver assistance systems and automated driving are known to strongly benefit from digital maps. Keeping map attributes up-to-date is a challenge especially for the current manual measuring approach. In this work we present methods to extract information about intersections and traffic lights through a crowdsourcing approach. We use position and dynamic data from a fleet of test vehicles with close-to-market sensors. A statistical hypothesis test is proposed to identify groups of driving directions at an entry of an intersection which have synchronous traffic light signaling. This information is used to improve the detection of the relevant traffic light signal in case that there is a different signaling for the driving directions. Based on a test dataset we classified whether the signaling is synchronous or not with an accuracy of 93.8 percent. To assess the usefulness of our mapping scheme, we have investigated its contribution to a camera-based traffic light recognition system. An evaluation of the use of additional map information for the traffic light detection was performed on a set of 344 logged intersection crossings from this vehicle. We showed that there is an improvement in the accuracy up to 5.2 percent dependent on the test conditions.**

I. Introduction

DIGITAL maps are one of the key components for future driver assistance systems and for highly automated driving. In current series systems maps are already used, e.g. to provide a foresight on upcoming speed limits and road slopes. A foresight assistant calculates ideal points where the driver should lift his foot off the accelerator pedal so that the car slows down and reaches the speed limit with the appropriate velocity. Visual hints to the driver at these points help to improve fuel efficiency.

Intersections are among the most complex traffic areas. Prior information from maps like the right of way and details about traffic lights are used in urban highly automated driving projects like [1]. However such map attributes are not included in state of the art digital maps. For research projects the attributes are generated in a manual or semi-automatic manner with specially equipped measurement cars. In the same way current digital maps for navigation are generated. These maps get an update approximately every three months wherein only parts of the map are updated. Map attributes have to be reliable and up-to-date for the utilization in safety critical applications like highly automated driving. This generates prohibitive effort especially with the state of the art approach of manual mapping.

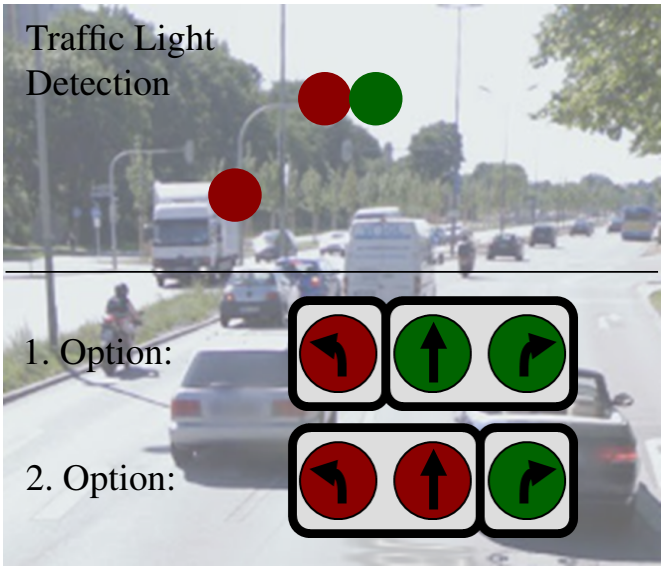

Fig. 1. Example of detected signals for a vehicle approaching an intersection. In case of crossing the intersection straight there are two options for the relevant signal. Streetview image: Google.

Besides the generation of up-to-date digital maps, another remaining challenge in the research of driver assistance systems is the reliable detection of the relevant traffic light signal. This task is particularly hard, when different traffic lights govern the individual driving directions at intersections. Functional requirements involving a detection range of at least $70\,\mathrm{m}$ where arrows on the lights are not yet resolved, pose additional challenges.

This contribution focuses on automated mapping methods for intersections. GPS traces complemented by dynamics data from a fleet of test vehicles close to series production are utilized to generate the map information. A database with $31\,000$ hours of test drives from $271\,458$ intersection crossings was set up for development and evaluation. The paper is based on previous work [2] where we introduced a method to infer stop line positions at intersections with traffic lights. Based on this we infer driving corridors, traffic light cycle times and information about synchronous traffic light signaling for pairs of possible turn maneuvers. The meaning of a synchronous signaling is that all signal phases start and end at the same time. We show the usefulness of this information

C. Ruhhammer, M. Baumann, V. Protschky and H. Kloeden are with BMW Group, D-80788 Munich, Germany.

F. Klanner is with Nanyang Technological University, Singapore 639798.

C. Stiller is with Karlsruhe Institute of Technology, Institute for Measurement and Control, D-76131 Karlsruhe, Germany.

at the example of improving a camera based traffic light recognition system mounted in a vehicle. Prototypic traffic light recognition systems based on preceding research [3], [4], [5], [6] are already available.

Figure 1 shows an example of detected signals at an intersection entry. A camera based traffic light recognition system is able to detect the color and position of every single signal relative to the car. The decision which of the signals is relevant is a challenging task. In case of the observed signal pattern red-red-green in Figure 1 there are two options for the relevant signal of a straight crossing. This situation can be resolved by utilizing up-to-date map information about groups of driving directions with synchronous signaling. Furthermore, in case that intersections are close to each other and in the range of the camera system, additional map information can be used to find the relevant light in longitudinal direction.

The remaining parts of the paper are structured as follows. After an overview of the related work in Section II, we introduce a method to extract a representation of the geometry and topology of intersections out of this data in Section III. This special description of intersection structures is necessary because current digital maps do not contain an appropriate representation for intersection specific properties.

The basic idea behind the work is to compare green times of the signaling from different driving directions at an intersection and to decide whether there are groups of driving directions with synchronous signaling. As the data only contains position and velocity information from vehicles, we infer a green signal state of traffic lights from the movement patterns over learned stop lines which is described in Section IV.

Our data is sparse with regards to time, so green signal observations from different driving directions at an intersection entry at the same time are rare. Therefore we exploit the fact that almost all traffic lights work with fixed cycle durations which means that they repeat their program after a certain time range. With the knowledge of the correct cycle duration it is possible to convolve all green signal observations into one cycle. The proposed method to extract the cycle duration is introduced in Section V. The convolved green observations make it possible to compare different driving directions in order to infer signal groups, which is described in Section VI and evaluated in Section VII.

The information about signal groups is utilized to support the detection of the relevant traffic light signal if different signals are detected by a camera system. Considering the situation in Figure 1, it is possible to infer the correct relevant signal for going straight with map information about the grouping of signals. The improvements on detecting the correct signal are evaluated in Section VII.

II. Related Work

Automatic mapping through crowd sourcing as a possibility to reduce the effort for generating digital maps was already investigated in [7], [8], [9], [10], [11], [12]. By utilizing cars with a connection to the internet as probe vehicles it is possible to automatically generate static and also dynamic map information like

- lane geometries and boundaries,
- (dynamic) speed limit information,
- road works information,
- road topologies for tactical decisions,
- descriptions of intersections

and even more.

Another approach of utilizing GPS traces to create maps through crowd sourcing is the OpenStreetMap (OSM) initiative [13]. OSM distributes freely available worldwide geographic map data. Through the contribution of a vast number of volunteers, OSM is one of the most detailed maps available today.

More recent work with regards to mining GPS traces includes the automatic classification of right of ways at intersections like in [10]. The authors present a rule-based approach to detect driving directions at intersections regulated by stop signs and traffic lights. They propose to use the information for navigation purposes. Furthermore, a supervised learning approach to classify traffic lights and stop signs with crowd sourced data is presented in [11]. The generated information about the location of intersections with traffic lights is relevant for urban driver assistance systems. Digital maps already contain partial information on the right of way. In our work we use such information from state-of-the-art maps, e.g. the location of intersections with traffic lights.

Besides the generation of map information there are also different research projects about assistance systems at intersections. One example is proposed in [14] where the vehicle is able to detect cross traffic, traffic signs and traffic lights. The driver gets a warning in case a conflict with other traffic participants or a violation of traffic rules is predicted. The system is also based on a digital map with detailed information about traffic lights and intersection topologies. However the map attributes are generated in a manual manner which is not scalable for series systems.

In [15] the authors propose a system to automatically map the three dimensional absolute positions of signalers from traffic lights and their corresponding driving direction. They utilize a special measurement car with a high precision localization and a traffic light detection system. In the mapping pipeline they also use humans to tweak the mapped data. After the pipeline about $1 - 5\,\%$ of traffic lights are still missing depending on the area and the traffic during the measurement. The reason is that a single measurement drive is used to extract the information. In this way it was possible to create a map with about one thousand intersections and over $4\,000$ lights. A camera based system utilizes the map to improve the detection of the correct signal. The aim of the map is to increase the detection range of the camera system while keeping false positives low through location based filtering. Tests showed that they reached a detection rate of almost $100\,\%$ up to $100\,\mathrm{m}$ in front of the traffic light. The accuracy is still at about $90\,\%$ at a range of $160\,\mathrm{m}$ and at about $75\,\%$ at $200\,\mathrm{m}$. However the paper does not propose a concept for selecting the relevant signal in case of different signal groups. The method to create the map requires manual work and measurement drives with specially equipped cars. This makes the updating process in a series system expensive and time consuming.

III. Representation of an Intersection

In order to be able to apply the developed methods independently on different geometries, we introduce a generic model for describing an intersection. The basic idea is that an intersection has entries and exits where cars enter and leave the area of an intersection. The possible combinations of entries and exits result in intersection paths. The following steps for generating a representation of an intersection are described in this section:

- Extraction of intersection entries and exits,
- Logical combination of entries and exits to determine possible paths through the intersection
- and generation of mean intersection paths.

Basis for the methods are intersection center points which are extracted from OSM by clustering intersection nodes with DBSCAN [16]. For every intersection we cut the GPS traces of recorded test drives into single intersection crossings within 70 m around the center. In the following the set of GPS traces $\mathcal{T}$ encodes the trajectories of traversals across the considered intersection. A trace $\xi_i \in \mathcal{T}$ consists of a set of n_i measurements $m_j^{(i)}$. Every single measurement $m_j^{(i)}$ of a trace with $j = 1, \dots, n_i$ is a tuple of a two dimensional position $\mathbf{x}_j^{(i)} \in \mathbb{R}^2$, a velocity $v_j^{(i)} \in \mathbb{R}$, a heading $\varphi_j^{(i)} \in [0, 2\pi)$ and an absolute time $t_j^{(i)} \in \mathbb{R}$, so $\xi_i = \{m_j^{(i)} | m_j^{(i)} = (\mathbf{x}_j^{(i)}, v_j^{(i)}, \varphi_j^{(i)}, t_j^{(i)})\}$. The time difference between two measurements is one second, so $t_{j+1}^{(i)} - t_j^{(i)} = 1\,\mathrm{s}$.

A. Extracting intersection entries and exits

The sets of entries $\mathcal{E}$ and exits $\mathcal{A}$ of an intersection are defined as a tupel of a position $\mathbf{x} \in \mathbb{R}^2$ and a direction $\varphi \in [0, 2\pi)$, so $\mathcal{E} = \{e | e = (\mathbf{x}_e, \varphi_e)\}$ and $\mathcal{A}$ is defined respectively. To get entries and exits, the first measurements $m_1^{(i)}$ respectively the last measurements $m_{n_i}^{(i)}$ of the intersection crossings are extracted from every GPS trace $\xi_i \in \mathcal{T}$. After applying a clustering algorithm separately on all first points of every trace and last points, the entry and exit locations are defined as the resulting cluster centers. Due to the huge spatial and temporal variations of noise in the GPS localization, density-based clustering methods, like e.g. DBSCAN [16] suffer from the challenge in the estimation of their hyperparameters.

Therefore K-means clustering is applied whereat the number of entries and exits is determined based on the probability distribution of the heading $f_1(\varphi)$ when entering or $f_{n_i}(\varphi)$ when exiting the intersection. To cope with heading noise the distribution is approximated through a kernel-density-estimator. Considering the circular characteristics of the heading, the number of the local maxima $K = |\{\varphi_k | f'(\varphi_k) = 0\}|$ of the distribution corresponds to the number of entries respectively exits. According to the determined number K of clusters we apply K-means clustering to the data points with the two dimensional position and the heading as features. To account for the circular characteristics of the heading, this feature is split into the sine and cosine values. A feature vector $\mathbf{f}_{\mathcal{E}}^{(i)}$ for the K-means clustering of entries $\mathcal{E}$ for example is extracted from the first measurements $m_1^{(i)}$ of every trace $\xi_i \in \mathcal{T}$, so $\mathbf{f}_{\mathcal{E}}^{(i)} = (\mathbf{x}_1^{(i)}, \sin(\varphi_1^{(i)}), \cos(\varphi_1^{(i)}))$. The feature vector $\mathbf{f}_{\mathcal{A}}^{(i)}$ for the clustering of exits $\mathcal{A}$ is extracted from the last measurements $m_{n_i}^{(i)}$ of the traces respectively.

Fig. 2. Entries and exits of an example intersection. Entries are marked with blue circles, exits are red. Additionally the corresponding entry and exit points of the traces are marked in the same color whereas outliers are grey. The GPS traces are cutted within 70 m around the center. As the traces consist of discrete measurements with a time difference of one second, the start and end points of a trace might be closer to the center than 70 m.

To filter outliers we apply a principal component analysis on the points of a resulting cluster and exclude points whose Mahalanobis distance to the cluster center exceeds a threshold. The position $\mathbf{x}$ and the orientation φ of each intersection entry or exit is determined by the cluster means. Every point in a cluster corresponds to a trace, since every trace can be assigned to an entry and an exit or considered as an outlier trace. Figure 2 shows the sets of entries $\mathcal{E}$ and exits $\mathcal{A}$ at an example intersection. For every entry $e \in \mathcal{E}$ and every exit $a \in \mathcal{A}$ the set of traces assigned to e or a is denoted as $\mathcal{T}_e$ and $\mathcal{T}_a$ respectively.

B. Mean intersection paths

Every pair (e, a) of an entry $e \in \mathcal{E}$ and an exit $a \in \mathcal{A}$ with at least one common trace results in an intersection path ρ_{ea}. Therefore the index set $\mathcal{I}$ for a set of paths is given by

$$\mathcal{I} = \{(e, a) | \mathcal{T}_e \cap \mathcal{T}_a \neq \emptyset, e \in \mathcal{E}, a \in \mathcal{A}\}. \tag{1}$$

From the corresponding set of traces, a mean intersection path is generated for every possible combination (e, a). A mean path ρ_{ea} of length n is defined as a sequence of points $\langle \mathbf{p}_0, ..., \mathbf{p}_n \rangle$, $n \geq 1$ where $\mathbf{p}_0 = e$ and $\mathbf{p}_n = a$. For a total order of the points we define that the euclidean distance $d(\cdot, \cdot)$ between two preceding points is lower than the distance to all following points

$$d(\mathbf{p}_k, \mathbf{p}_{k-1}) \leq d(\mathbf{p}_k, \mathbf{p}_{k+l}), \tag{2}$$

where $1 \leq k \leq n-1$ and $k+1 \leq l \leq n$.

Through projecting a position value on a mean path ρ_{ea}, we get a longitudinal position offset along the mean path. The root of the coordinate system is the projected intersection center. The complexity of our developed methods for processing position data decreases by reducing the dimensionality. Additionally the projection does not impose any assumptions on the geometry of intersections. This supports the design of generic algorithms on the data.

We apply the mean shift clustering method [17] to all position values $\mathbf{x}_j \in \mathcal{X}_{ea}$ of the traces with the entry e and exit a to generate mean paths. This method estimates the local gradient of an arbitrary data distribution. The first step of the approach is to calculate the mean $\bar{\mathbf{x}}$ on a subset of the two dimensional position values $\mathcal{X}_{ea}$ of all traces $\mathcal{T}_{ea} = \mathcal{T}_a \cap \mathcal{T}_e$ of a path ρ_{ea}. The subset is created by applying a flat kernel $K(\mathbf{x}_j - \mathbf{c}_1^{(i)})$ on all positions $\mathbf{x}_j \in \mathcal{X}_{ea}$ at an arbitrary center point $\mathbf{c}_1^{(i)} \in \mathcal{X}_{ea}$. So the mean $\bar{\mathbf{x}}(\mathbf{c}_1^{(i)})$ is given by

$$\bar{\mathbf{x}}(\mathbf{c}_1^{(i)}) = \frac{\sum\limits_{\mathbf{x}_j \in \mathcal{X}_{ea}} \mathbf{x}_j K(\mathbf{x}_j - \mathbf{c}_1^{(i)})}{\sum\limits_{\mathbf{x}_j \in \mathcal{X}_{ea}} K(\mathbf{x}_j - \mathbf{c}_1^{(i)})} \tag{3}$$

with

$$K(\mathbf{y}) = \begin{cases} 1 & \text{if } \|\mathbf{y}\|_2 \leq \lambda \\ 0 & \text{if } \|\mathbf{y}\|_2 > \lambda \end{cases}. \tag{4}$$

The utilization of the flat kernel results in a mean where only data points within a distance of $\lambda \in \mathbb{R}$ around $\mathbf{c}_1^{(i)}$ are considered. The vector $\bar{\mathbf{x}}(\mathbf{c}_1^{(i)}) - \mathbf{c}_1^{(i)}$ approximates the gradient of the distribution at $\mathbf{c}_1^{(i)}$. By applying the method iteratively with $\mathbf{c}_{j+1}^{(i)} = \bar{\mathbf{x}}(\mathbf{c}_j^{(i)})$, the center reaches a local maximum $\mathbf{c}_{\max}^{(i)}$ of the density of the distribution. After a restart with a different start value $\mathbf{c}_1^{(i+1)} \in \mathcal{X}_{ea}$, we get an additional maximum $\mathbf{c}_{\max}^{(i+1)}$. The maxima are ordered according to equation (2). To remove outliers of the density maxima, we test the feasibility of every local maximum based on the direction change related to the previous maximum. Given the orientation vectors $\mathbf{o}_{i-1} = \mathbf{c}_{\max}^{(i)} - \mathbf{c}_{\max}^{(i-1)}$ and $\mathbf{o}_i = \mathbf{c}_{\max}^{(i+1)} - \mathbf{c}_{\max}^{(i)}$, $\mathbf{c}_{\max}^{(i)}$ is considered as an outlier if $\arccos(\mathbf{o}_{i-1} \cdot \mathbf{o}_i) > \frac{\pi}{2}$. A discretized cubic interpolation of the remaining center points yields to the mean path $\rho_{ea}(\lambda) = \langle \mathbf{p}_0, ..., \mathbf{p}_n \rangle$ with the distance parameter λ of the flat Kernel as parameter.

The advantages of this non-parametric method over parametric regression are that no assumption about the shape of the path is necessary and λ is the only parameter that needs to be determined. As the noise level of the position values varies at different intersections, different values for λ are appropriate. The λ parameter defines the width of the kernel which should be low to get a good approximation of the real mean path. However, given noisy data a low λ leads to outliers. The formulation of an optimization problem helps to tackle this trade-off. A suitable representation of the mean path is found when the aggregated distance of all points to the path is minimal. The lateral distance of a position value $\mathbf{x}_j \in \mathcal{X}_{ea}$ to a path is calculated with a given distance function

$$\text{dist}\colon \mathbb{R}^2 \times \mathcal{P} \to \mathbb{R} \tag{5}$$

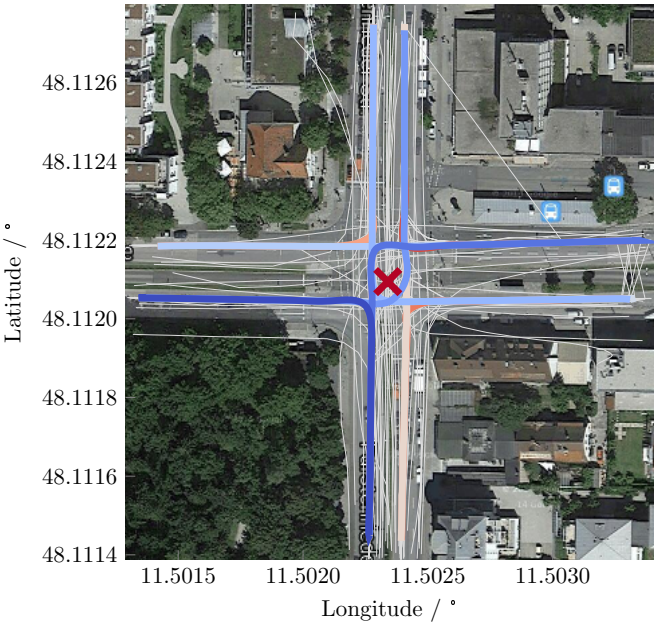

Fig. 3. Mean paths of the example intersection. The red cross represents the intersection center extracted from OpenStreetMap.

which takes a point $\mathbf{x} \in \mathbb{R}^2$ and a polyline $\rho_{ea}(\lambda) \in \mathcal{P}$ as inputs. Therefore, the optimal parameter λ_{opt} is calculated by

$$\lambda_{\text{opt}} = \arg\min_{\lambda \in \mathbb{R}} \sum_{\mathbf{x}_j \in \mathcal{X}_{ea}} \text{dist}(\mathbf{x}_j, \rho_{ea}(\lambda)). \tag{6}$$

We choose the minimal distance of a position value $\mathbf{x}_j \in \mathcal{X}_{ea}$ to every point of the polyline $\rho_{ea}(\lambda) \in \mathcal{P}$ as distance:

$$\text{dist}(\mathbf{x}_j, \rho_{ea}(\lambda)) = \min_{\mathbf{y}_j \in \rho_{ea}(\lambda)} \|\mathbf{x}_j - \mathbf{y}_j\|_2. \tag{7}$$

Position values which are further away from the first estimation of the mean path than the median of the distances of all positions are filtered. A new mean path is generated based on the remaining points to get an improved second estimate. The resulting mean intersection paths through the example intersection is shown in Figure 3. After projecting the two-dimensional position coordinates onto the mean paths, the approach presented in [2] is applied to estimate stop line positions based on the spatio-temporal information in each trace. In summary, an intersection is characterized by

- an intersection center,
- entries,
- exits,
- mean intersection paths,
- and stop line positions for every path.

The following work is based on this intersection description.

IV. Inferring Traffic Light Signal States from Fleet Data

In this section a method is proposed to extract a set of m observations of a green signal state of a traffic light $\mathcal{G}_i = \{t_{\text{g}}^{(j)}, ..., t_{\text{g}}^{(m)}\}$ from a trace $\xi_i \in \mathcal{T}_{ea}$, where $t_{\text{g}}^{(j)} \in \mathbb{N}$ are defined as UNIX timestamps in seconds. The aim is to collect

TABLE I
PARAMETERS OF THE WAITING QUEUE MODEL AT STOP LINES

Parameter	T_{R_1}	T_{R_f}	D_{S_1}	L_{S}
Value	1.3 s	1.0 s	1.0 m	6.5 m

green observations $\mathcal{G}_{ea}$ for every path ρ_{ea} of an intersection which are defined as the disjoint union

$$\mathcal{G}_{ea} = \bigsqcup_{i \in [1,n]} \mathcal{G}_i \tag{8}$$

of the observations of all traces $\xi_i \in \mathcal{T}_{ea}$ assigned to the path with $n = |\mathcal{T}_{ea}|$.

First we extract the time $t_{\mathrm{S}}(\xi_i)$ of passing the stop line from a trace ξ_i. Assuming that all drivers follow the traffic regulations, we get a green signal observation for the time of passing the stop line. The observation model distinguishes traces without a stop from traces with a stop. The minimum duration of a green signal phase is five seconds according to the regulations for traffic lights RiLSA [18] in Germany. Therefore we can observe a set of green signals $\mathcal{G}_i = \{t_{\mathrm{S}}(\xi_i) - 4\,\mathrm{s}, t_{\mathrm{S}}(\xi_i) - 3\,\mathrm{s}, ..., t_{\mathrm{S}}(\xi_i)\}$ for every trace $\xi_i \in \mathcal{T}_{ea}^{\mathrm{nostop}}$ of a path without a stop.

Vehicles which stop close to the stop line pass it in less than five seconds after the start of a green phase. Therefore we introduce a separate observation model for vehicle traces $\xi_j \in \mathcal{T}_{ea}^{\mathrm{stop}}$ with a stop before passing the stop line. The aim of this model is to estimate the switch time from red to green based on the start time after a stop. We use a waiting queue model [19] with the distance $d_{\mathrm{S}}(\xi_j)$ to the stop line and the absolute start time $t_{\mathrm{Start}}(\xi_j)$ after a stop as inputs. The start time $t_{\mathrm{Start}}(\xi_j)$ is extracted from the velocity profile. The time range Δt_j from the signal transition until the start of driving depends on the position of the observed vehicle in the waiting queue as the reaction times of the drivers before sum up. Thereby the reaction time T_{R_1} of the first driver in the row is larger on average compared to the reaction time T_{R_f} of following drivers. The reason is that following drivers are able to prepare the start. To compute the total reaction time, we estimate the number of vehicles in the waiting queue in front of the observed vehicle by utilizing a mean distance D_{S_1} of the first vehicle and a mean total length L_{S} from vehicle front to the next vehicle front. The parameters of Table I are estimations which follow investigations about driver behavior at intersections with traffic lights [20]. With the estimated time difference Δt_j from signal transition to the start of driving

$$\Delta t_j = T_{\mathrm{R}_1} + \frac{d_{\mathrm{S}}(\xi_j) - D_{\mathrm{S}_1}}{L_{\mathrm{S}}} \cdot T_{\mathrm{R}_f} \tag{9}$$

we get the estimated absolute start of the green phase $t_{\mathrm{G}}(\xi_j)$ as follows:

$$t_{\mathrm{G}}(\xi_j) = t_{\mathrm{Start}}(\xi_j) - \Delta t_j. \tag{10}$$

The set of green signal observations for every trace $\xi_j \in \mathcal{T}_{ea}^{\mathrm{stop}}$ with a stop is generated based on the start of green and the time of passing the stop line $\mathcal{G}_j = \{t_{\mathrm{G}}(\xi_j), ..., t_{\mathrm{S}}(\xi_j)\}$.

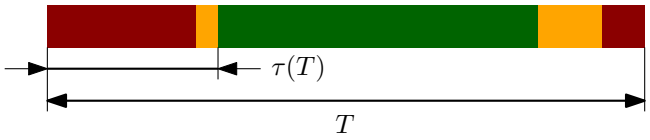

Fig. 4. The relative green start time $\tau(T)$ within a cylce T of an examplary traffic light signaling cycle.

V. CYCLE DURATION ESTIMATION OF TRAFFIC LIGHTS

As already mentioned in Section I, knowledge of the cycle duration of traffic lights is a prerequisite for the extraction of signal groups. The cycle duration T is the time between two servings of each signal group. The start of a cycle is defined by the multiple of the cycle duration beginning at a certain reference time. In this work, the reference time is defined to 00:00 on January 1st 1970 which corresponds to the UTC reference time, whereat the local current time is considered. The relative time τ within a cycle T can be calculated through a modulo operation on a time t relative to the reference time:

$$\tau(T) = \mathrm{mod}(t, T). \tag{11}$$

The parameters are represented in Figure 4. According to the RiLSA [18], possible values for a cylce time are defined as integers between 30 s and 120 s, which yields a set of cycle time hypotheses $T \in \mathbb{N}$ and $T \in [30\,\mathrm{s}, 120\,\mathrm{s}]$. By estimating the correct cycle duration it is possible to transform all absolute green signal observations into one cycle. This is a prerequisite to estimate the green phase for the signaling of different paths as our data is sparse in time.

A. Previous work on cycle duration estimation of traffic lights

Cycle duration estimation from vehicle traces has already been investigated in some previous research projects. In [21] the authors estimate the beginning of a green signal phase and calculate the difference of consecutive estimations. The cycle duration is estimated through solving an optimization problem where the difference between the green start time intervals and a multiple of the cycle duration is minimized. This approach causes errors on wrong multiples of the correct cycle duration.

In [22] the authors assume that there are no temporal-spatial conflicting traces of different intersection paths. For every possible value of the cycle duration, a test is applied if there exists at least one conflict. Every cycle duration which produces conflicts is discarded. Therefore the approach is not robust against measurement inaccuracies of the position and time data.

Based on the results and findings of the approach presented in this work, we had investigated three more approaches in [23] to estimate the correct cycle duration of traffic lights. The approaches use cyclic features of the traces like stopping times or the pairwise correlation coefficient between the complete spatial-temporal movement patterns. Another approach is based on image processing methods where the spatial-temporal movement patterns of all traces yield to a two dimensional image for every estimated cycle duration. A region growing algorithm finds regions of time and location without observed

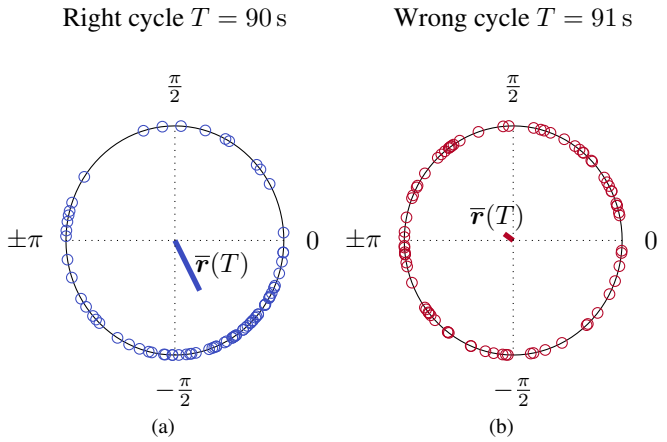

Fig. 5. Projection of green start times $t_{\mathrm{G}}(\xi_j)$ on a unit circle through the transformation into an angle $\alpha_j(T)$ for different cycle time estimates. The variation of the angles is represented through the mean direction $\overline{\boldsymbol{r}}(T)$. The mean direction is more distinctive for the correct cycle duration $T_{\mathrm{cyc}} = 90\,\mathrm{s}$.

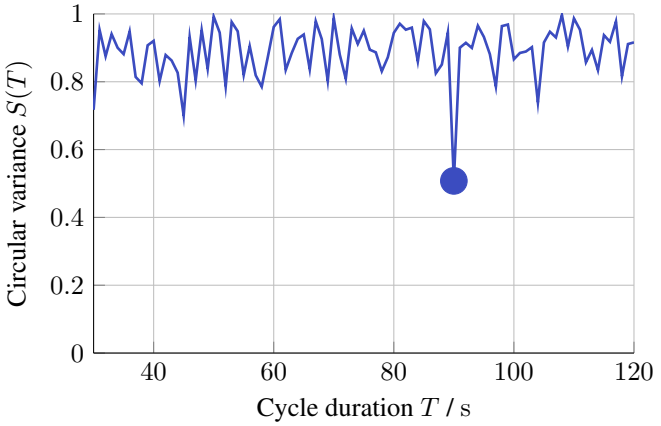

Fig. 6. Circular Variance $S(T)$ dependent on discrete values of the cycle duration T. The circular variance has a global minimum at the correct cycle duration $T_{\mathrm{cyc}} = 90\,\mathrm{s}$. The Hodges-Ajne test with a p-value of $p = 0.001$ shows that only the value for the correct cycle duration is significantly different to a uniform distribution.

crossing data. The larger the regions, the more likely is the correct estimation of the cycle duration as the spatial-temporal patterns spread for incorrect cycle durations. The evaluation results in [23] indicate that fusing different methods yields to the best result but the methods are computationally expensive.

B. Cycle duration estimation approach: Circular Variance

In this work we propose an additional approach for estimating the cycle duration. The method is based on minimizing the circular variance of estimated start times of the green signal phase $t_{\mathrm{G}}(\xi_j)$ with $j = 1...k$ from k intersection traces $\xi_i \in \mathcal{T}_{ea}^{\mathrm{stop}}$ with a stop according to Equation (10).

In circular statistics data is projected on a unit circle as an angle α [24]. The estimated absolute green start times $t_{\mathrm{G}(\xi_j)}$ are transformed into relative times $\tau_j(T)$ for every cycle time hypothesis T according to Equation (11). Then the relative times are converted to angles

$$\alpha_j(T) = 2\pi \frac{\tau_j(T)}{T}. \tag{12}$$

The first step to determine the variance of circular data is to calculate the mean direction

$$\overline{\boldsymbol{r}}(T) = \frac{1}{n}\sum_{j=1}^{n} \boldsymbol{r}_j(T), \text{ with } \boldsymbol{r}_j(T) = \begin{bmatrix} \cos\left(\alpha_j(T)\right) \\ \sin\left(\alpha_j(T)\right) \end{bmatrix} \tag{13}$$

from n data points. Figure 5a shows the projected green start times and the resulting mean direction for the correct cycle duration $T = 90\,\mathrm{s}$ based on data from real intersection crossings. The transformed observations of the green start time $\alpha_j(T)$ are concentrated on a limited part of the circle. There are some outliers mainly because of measurement inaccuracies or changes of the signal program and cycle durations. Applying the transformation with a wrong cycle duration as shown in Figure 5b results in scattering observations over the complete circle. The absolute value of the mean direction is significantly lower in this case.

We use the resulting mean direction to estimate the circular variance [24]

$$S(T) = 1 - \|\overline{\boldsymbol{r}}(T)\|_2 \tag{14}$$

of the green start times. Figure 6 shows the dependence of the circular variance on the cycle duration for real traces from an intersection. Out of the data we determine the stop line position [2] and applied the observation model to estimate green start times. According to the RiLSA [18], the set of allowed cycle durations is defined as $\{T \in \mathbb{N} | 30\,\mathrm{s} \leq T \leq 120\,\mathrm{s}\}$. The circular variance has a global minimum at the correct cycle duration $T_{\mathrm{cyc}} = 90\,\mathrm{s}$. Hence the cycle duration is estimated as

$$T_{\mathrm{cyc}} = \underset{\{T \in \mathbb{N} | 30\,\mathrm{s} \leq T \leq 120\,\mathrm{s}\}}{\arg\min} S(T). \tag{15}$$

Some types of traffic lights adapt their cycle duration throughout the day due to varying traffic volume. The detection of these adaptions improves the result with regard to the determination of signal groups and therefore is currently ongoing work. Green start times from other cycle durations cause more noise in the following methods. Nevertheless it is possible to find the most significant cycle duration even without the knowledge of the adaptions by applying a significance test on the global minimum of the circular variance. We utilize the Hodges-Ajne test [25], a hypothesis test for circular uniformity, with a p-value of $p = 0.001$. For the example in Figure 6, the uniformity hypothesis is only rejected for the correct cycle duration $T_{\mathrm{cyc}} = 90\,\mathrm{s}$.

VI. Extracting Groups of Directions with Synchronous Signaling

Knowledge of the correct cycle duration of a traffic light, allows to map all observations into one cycle according to Equation (11). With the observations, a multinomial distribution which represents the probability $P(\tau|R_i)$ for a given green observation to occur at the relative time τ, given a driving direction $R_i \in \{\text{left, straight, right}\}$ is estimated.

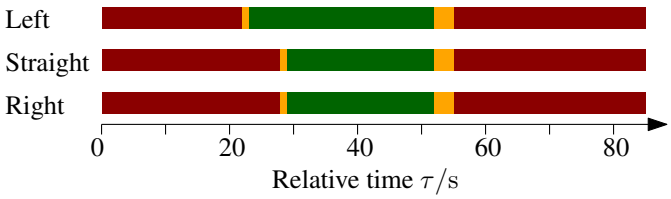

Fig. 7. Signaling of different driving directions with $T_{\mathrm{cyc}} = 85\,\mathrm{s}$.

To determine signal groups we compare these distributions pairwise and classify them as synchronous or not.

For the development of the following methods an exemplary intersection was simulated with the microscopic traffic simulation SUMO [26]. The advantage of the simulation is that parameters like the number of intersection traces and the noise of the measurements are easy to adapt. A single intersection entrance is simulated whereat the signaling for turning left ist not synchronous to going straight but the signaling for turning right is synchronous to going straight.

Figure 7 shows the traffic light signaling of the simulation for every driving direction. We simulate the traffic at the intersection entry with a traffic flow of 350 vehicles per hour for every driving direction. 50 intersection traces are selected randomly and used for further processing steps. Relative green signal observations are extracted from the traces based on the simulated cycle duration of $T_{\mathrm{cyc}} = 85\,\mathrm{s}$. There are 494 observations of a green signal on average for every driving direction. $20\,\%$ of the simulated observations are chosen randomly and spread uniformly over the time of one day, as the measurements are noisy in the real data set. The result are arbitrary observations of a green signal.

Figure 8 shows the distributions of relative green start times of three driving directions for a simulated cycle duration of $T_{\mathrm{cyc}} = 85\,\mathrm{s}$. Comparing the distributions we determine if different driving directions are regulated by a synchronous signaling. In addition to a new distance measure for the comparison which is introduced later, we calculate the known distance measures "Kullback-Leibler-Divergence" (KL) [27] and "Earth Mover's Distance" (EMD) [28] as baseline approaches. The KL between the probability distributions of two driving directions R_1 and R_2 is calculated by

$$\mathrm{KL}\left(P\left(\tau|R_1\right), P\left(\tau|R_2\right)\right) = \sum_{\mathfrak{t}\in[1,T_{\mathrm{cyc}}]} P(\mathfrak{t}|R_1) \cdot \log\frac{P(\mathfrak{t}|R_1)}{P(\mathfrak{t}|R_2)}. \tag{16}$$

The EMD is determined by the iterative algorithm:

1: $e_0 = 0$
2: $e_{\mathfrak{t}} = P(\mathfrak{t}|R_1) + e_{\mathfrak{t}-1} - P(\mathfrak{t}|R_2)$
3: $\mathrm{EMD}\left(P\left(\tau|R_1\right), P\left(\tau|R_2\right)\right) = \sum_{\mathfrak{t}\in[1,T_{\mathrm{cyc}}]} |e_{\mathfrak{t}}|$.

Additionally we propose a new distance measure based on Bayes' rule which takes domain specific properties of the distributions into account. The characteristics of a separated signaling differ significantly. In the example in Figure 7 the green signal phases overlap for 23 s. Only the start of the green phase differs by five seconds. In reality, a difference of the signaling for the two driving directions regarding the start time or the end time or both is possible. Another possibility

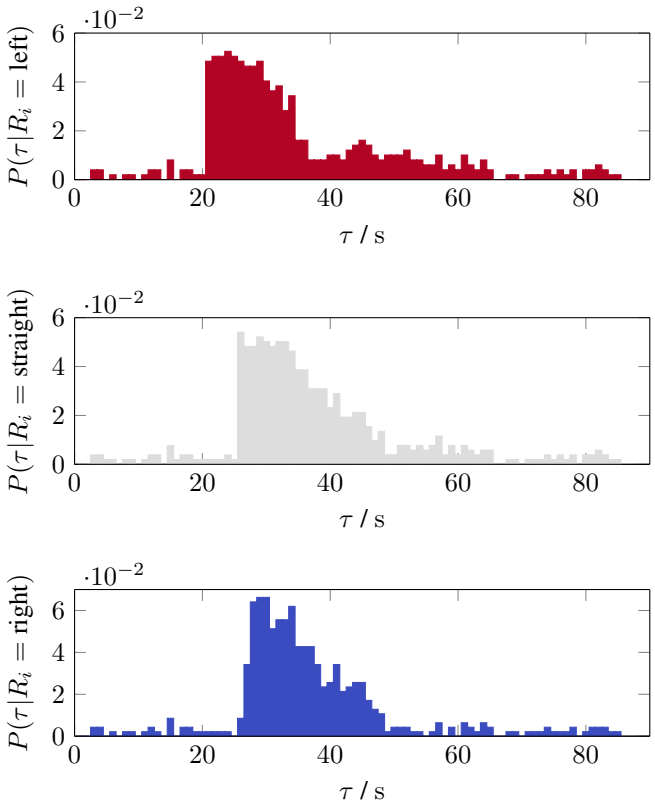

Fig. 8. Simulated multinomial distributions of green observations for different driving directions of the simulated intersection entry with a cycle duration $T_{\mathrm{cyc}} = 85\,\mathrm{s}$.

is that there is no overlap between the green phases. In cases of overlapping distributions in a wide time range it is most difficult to classify a separated signaling. In this case, the known distance measures from the literature give a similar value compared to cases with synchronous signaling. Therefore we define a new distance measure based on a Bayesian model comparison [29, chapter 12] and evaluate the measure against KL and EMD in Section VII. The developed method consists of the following steps:

- Probabilistic Bayesian comparison of the distributions of green observations for every second of the cycle
- Circular smoothing of the comparison result
- Setting the distance measure to the minimum of the smoothed comparison result

A. Probabilistic comparison of the distributions of green observations with the Bayes factor

The developed measure proposed in this contribution is based on comparing the binomial distributions of green observations for every second within a cycle separately. For a driving direction R_i we get $z_{i,\tau} \in \mathbb{N}_0$ traces with a green observation at the relative time τ out of $n_i \in \mathbb{N}$ total traces. For two driving directions R_i with $i \in \{1, 2\}$ we get an observation vector $\mathbf{z}_\tau = [z_{1,\tau}, z_{2,\tau}]$. Let $\theta_{i,\tau} \in \mathbb{R}$ with $0 \leq \theta_{i,\tau} \leq 1$ denote the probability of a green observation for driving direction i at time τ for a single trace. A Bayesian hypothesis test is proposed to compare the probabilities of a

green observation for two driving directions at every time τ within a cycle. The two hypotheses are that the parameters $\theta_{1,\tau}$ and $\theta_{2,\tau}$:

- are equal, $\theta_{1,\tau} = \theta_{2,\tau}$ (null hypothesis)
- or non equal, $\theta_{1,\tau} \neq \theta_{2,\tau}$ (alternative hypothesis).

For the model selection approach, the probabilities of the observed data $\mathbf{z}_\tau$ given the models M_{null} and M_{alt} for the two hypothesis have to be derived as follows.

Initially we express the probability for the vector of observations by a product of binomial distributions:

$$P(\mathbf{z}_\tau|\theta_{1,\tau},\theta_{2,\tau}) = \prod_{i=1}^{2} \binom{n_i}{z_{i,\tau}} (\theta_{i,\tau})^{z_{i,\tau}} \cdot (1-\theta_{i,\tau})^{n_i - z_{i,\tau}}. \tag{17}$$

First the probability for the observed data $\mathbf{z}_\tau$ is derived for the alternative hypothesis. We start by applying Bayes rule on Equation (17) to get the probability for the unknown variables $\theta_{1,\tau}$ and $\theta_{2,\tau}$

$$P(\theta_{1,\tau},\theta_{2,\tau}|\mathbf{z}_\tau) = \frac{P(\mathbf{z}_\tau|\theta_{1,\tau},\theta_{2,\tau}) \cdot P(\theta_{1,\tau}) \cdot P(\theta_{2,\tau})}{P(\mathbf{z}_\tau)}. \tag{18}$$

The beta distribution is utilized as a non-informative prior to model the probabilities $P(\theta_{i,\tau})$ which is shown later. The main reason for this choice is that the beta distribution is a conjugate prior of the binomial distribution. The beta distribution $\text{Beta}(p,q)$ is given as follows:

$$P(\theta) = \begin{cases} \frac{\theta^{p-1}(1-\theta)^{q-1}}{B(p,q)} & \text{for } 0 \leq \theta \leq 1 \\ 0 & \text{otherwise} \end{cases} = \text{Beta}(p,q), \tag{19}$$

with the variables $p, q \in \mathbb{N}$ and the beta function

$$B(p,q) = \int_0^1 \theta^{p-1}(1-\theta)^{q-1}\, d\theta = \frac{\Gamma(p)\Gamma(q)}{\Gamma(p+q)} \tag{20}$$

as normalizing constant where Γ denotes the gamma function. The variables p and q represent initial knowledge about positive and negative observations. Equation (18) is rearranged to

$$P(\theta_{1,\tau},\theta_{2,\tau}|\mathbf{z}_\tau) = \frac{\prod_{i=1}^{2} \binom{n_i}{z_{i,\tau}} (\theta_{i,\tau})^{z_{i,\tau}+p_{i,\tau}-1} \cdot (1-\theta_{i,\tau})^{n_i - z_{i,\tau}+q_{i,\tau}-1}}{P(\mathbf{z}_\tau) \cdot B(p_{1,\tau},q_{1,\tau}) \cdot B(p_{2,\tau},q_{2,\tau})}. \tag{21}$$

Comparing the numerator in Equation (21) with the numerator of the beta distribution in Equation (19), it appears that $P(\theta_{1,\tau},\theta_{2,\tau}|\mathbf{z}_\tau)$ can also be expressed as multiplication of beta distributions $\text{Beta}(z_{i,\tau}+p_{i,\tau}, n_i - z_{i,\tau} + q_{i,\tau})$. In this case the denominator has to be a product of beta functions and therefore the probability for our observations is inferred to

$$P(\mathbf{z}_\tau) = \frac{\prod_{i=1}^{2} \binom{n_i}{z_{i,\tau}} B(z_{i,\tau}+p_{i,\tau}, n_i - z_{i,\tau} + q_{i,\tau})}{B(p_{1,\tau},q_{1,\tau}) \cdot B(p_{2,\tau},q_{2,\tau})}. \tag{22}$$

Utilizing Bayes model comparison [30, Section 7.4], driving directions R_i are compared for every second τ within a cycle based on the probability of observations. For the null hypothesis M_{null} we assume the parameters $\theta_{1,\tau}$ and $\theta_{2,\tau}$ to be equal:

$$M_{\text{null}} \rightarrow \theta_{1,\tau} = \theta_{2,\tau}. \tag{23}$$

The assumption of the alternative hypothesis M_{alt} is that the two parameters are different:

$$M_{\text{alt}} \rightarrow \theta_{1,\tau} \neq \theta_{2,\tau}. \tag{24}$$

For the alternative hypothesis a uniform a priori distribution of the parameter $\theta_{i,\tau}$ is given by a beta distribution $\text{Beta}(1,1)$. So the probability of the data is calculated by

$$\begin{aligned} P(\mathbf{z}_\tau|M_{\text{alt}}) &= \frac{\prod_{i=1}^{2} \binom{n_i}{z_{i,\tau}} B(z_{i,\tau}+1, n_i - z_{i,\tau}+1)}{B(1,1) \cdot B(1,1)} \\ &= \prod_{i=1}^{2} \binom{n_i}{z_{i,\tau}} B(z_{i,\tau}+1, n_i - z_{i,\tau}+1), \end{aligned} \tag{25}$$

with $B(1,1) = 1$.

The parameters $\theta_{1,\tau}$ and $\theta_{2,\tau}$ are equal for both driving directions under the null hypothesis. Therefore $P(\theta_{1,\tau},\theta_{2,\tau}) = 0$ for $\theta_{1,\tau} \neq \theta_{2,\tau}$. Given $\theta_{1,\tau} = \theta_{2,\tau} = \theta_\tau$, the probability of the data for the null hypothesis can be analytically calculated by the integral

$$\begin{aligned} P(\mathbf{z}_\tau|M_{\text{null}}) &= \int_0^1 P(\mathbf{z}_\tau|\theta_\tau)\, d\theta_\tau \\ &= \int_0^1 \prod_{i=1}^{2} \binom{n_i}{z_{i,\tau}} (\theta_\tau)^{z_{i,\tau}} \cdot (1-\theta_\tau)^{n_i - z_{i,\tau}}\, d\theta_\tau. \end{aligned} \tag{26}$$

According to the definition of the normalizing constant $B(p,q)$, the probability of the observed data for the null hypothesis is given by

$$\begin{aligned} P(\mathbf{z}_\tau|M_{\text{null}}) &= \binom{n_1}{z_{1,\tau}} \binom{n_2}{z_{2,\tau}} \\ &\quad \cdot B(z_{1,\tau}+z_{2,\tau}+1, n_1 - z_{1,\tau} + n_2 - z_{2,\tau}+1). \end{aligned} \tag{27}$$

The model comparison after Bayes is defined as

$$\frac{P(M_{\text{alt}}|\mathbf{z}_\tau)}{P(M_{\text{null}}|\mathbf{z}_\tau)} = \frac{P(\mathbf{z}_\tau|M_{\text{alt}})}{P(\mathbf{z}_\tau|M_{\text{null}})} \cdot \frac{P(M_{\text{alt}})}{P(M_{\text{null}})}. \tag{28}$$

If the a priori probability of both models is equal $P(M_{\text{alt}}) = P(M_{\text{null}}) = 0.5$, the so called Bayes factor [31]

$$BF = \frac{P(M_{\text{alt}}|\mathbf{z}_\tau)}{P(M_{\text{null}}|\mathbf{z}_\tau)} = \frac{\prod_{i=1}^{2} B(z_{i,\tau}+1, n_i - z_{i,\tau}+1)}{B(z_{1,\tau}+z_{2,\tau}+1, n_1 - z_{1,\tau} + n_2 - z_{2,\tau}+1)} \tag{29}$$

follows from Equations (25) and (27).

As at least one of the hypotheses is valid, we can add the condition $P(M_{\text{alt}}|\mathbf{z}_\tau) + P(M_{\text{null}}|\mathbf{z}_\tau) = 1$. So the probability for the null hypothesis M_{null} at a time τ within the cycle is

$$P(M_{\text{null}}|\mathbf{z}_\tau) = \frac{1}{1+BF}. \tag{30}$$

B. Circular smoothing of the comparison result and determining the distance measure

Single outliers resulting from deviations of the estimated stop line or measurement inaccuracies should not have a significant impact on the distance measure. Therefore we apply a circular smoothing on the resulting probability which is denoted as $p(\tau) = P(M_{\text{null}}|\mathbf{z}_\tau)$ for the null hypothesis with a circular convolution of a discrete Gaussian kernel $K_\sigma(x)$. The advantage of a Gaussian kernel over a classical sinc kernel is a strictly decreasing frequency response. Nevertheless we also utilized a sinc kernel experimentally which showed that the choice of the kernel has no significant impact on the results of the classification. The smoothed function $s(\tau)$ is calculated by

$$s(\tau) = \sum_{\mathfrak{t}=1}^{T} K_\sigma(\tau - \mathfrak{t}) \cdot p(\mathfrak{t}). \tag{31}$$

The σ parameter is set to $\sigma = 2.5\,\text{s}$, therefore it is possible to detect a minimal difference between the green phases of five seconds. The continuous line in Figure 9a shows that this requirement is fulfilled as the simulated signaling varies only in a range of five seconds. A concise decline of the smoothed result of the model comparison in the time range $\tau \in [21\,\text{s}, 25\,\text{s}]$ confirms the correct choice of the parameter.

The proposed distance measure d is defined as the minimum of the smoothed comparison result $s(\tau)$, which means it is the minimal probability for a synchronous signaling:

$$d = \min\left(s\left(\tau\right)\right). \tag{32}$$

Figure 9 shows the result of the model comparison for every second within the cycle independently as dashed lines. For the comparison of right and straight, the average probability for the null hypothesis is 0.86, which means that they probably have a synchronous signaling. There is one outlier at $\tau = 26\,\text{s}$ which can be explained by inaccuracies in the estimation of the stop lines for every driving direction which causes a shift of the green observations.

The comparison of left and straight results in low probabilities for a synchronous signaling within $\tau \in [21\,\text{s}, 25\,\text{s}]$ and $\tau \in [33\,\text{s}, 41\,\text{s}]$. The reasons are an earlier start of the green phase for turning left and therefore the queue of vehicles also passes the stop line earlier as we simulated an equal traffic flow. This results in less green observations a certain time after the start of green. There are almost no observations for both directions during overlapping red phases so the measured distributions are considered to be realizations of the same underlying distribution.

The resulting distance measures for both turning directions in comparison to going straight at the simulated intersection entry are marked by a dot in Figure 9. As the measure corresponds to a probability, the range of values is $d \in [0, 1]$. Due to the properties of the Bayesian model comparison, the value 1 will only be reached for an infinite number of samples. Therefore the proposed distance measure is not a metric. Compared to the distance measures known from literature, our measure has the advantage that we can define the desired difference range between the distribution with the smoothing parameter σ. Additionally the method is robust against outliers caused by measurement inaccuracies.

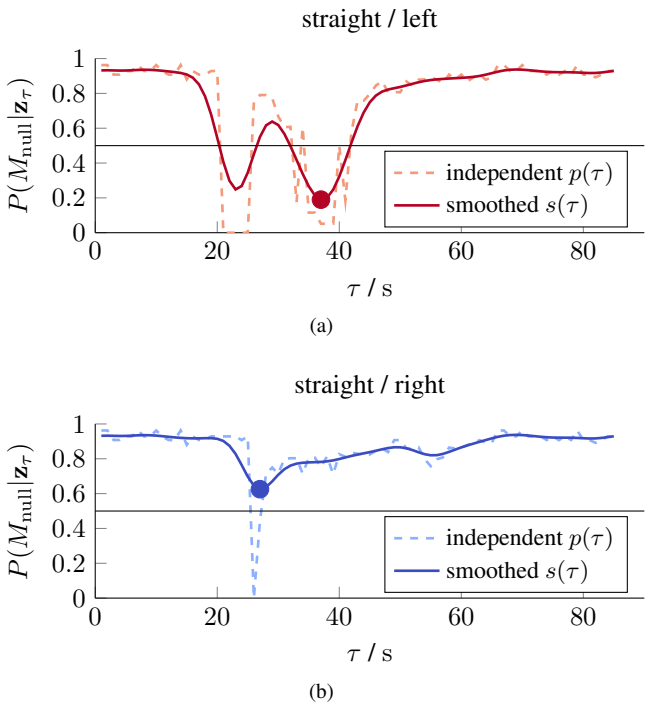

Fig. 9. Results of the Bayesian model comparison. The probability for the null hypothesis is the probability that a turning maneuver has synchronous signaling compared to going straight. The dashed lines represent the comparison result for every second of the cycle independently. The continuous lines are the smoothed result of the comparison.

VII. Experimental Results

An evaluation of the developed methods on extracting signal groups is performed on real data from test vehicles extracted from our database. Additionally we evaluate the improvements on detecting the relevant traffic light signal utilizing the signal group information on a set of 344 intersection crossings with a prototypic camera based traffic light detection system.

A. Evaluation of the extraction of signaling groups

For the evaluation of the extracted signal groups we identified pairs of intersection paths with the same intersection entry and enough traces to be able to estimate a stop line [2]. For these pairs, the grouping of driving directions is manually labeled utilizing Google StreetView. Our database contains 48 pairs of paths which fulfill the requirements where 17 pairs have different and 31 pairs have synchronous signaling.

After generating the representation according to Section III for every intersection, the stop line positions are estimated for every path. This information is used to generate observations of a green signal according to Section IV. Based on the estimated cycle duration of the traffic light we classify if there is synchronous signaling for different driving directions utilizing distance measures. The proposed distance measure is evaluated against the known measures from literature. Therefore a simple binary linear classifier is applied to the resulting different distances. By varying the threshold, a Receiver Operating

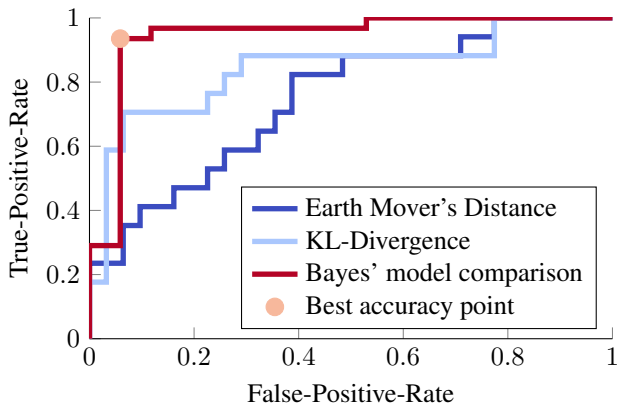

Fig. 10. Receiver Operating Characteristic for detecting groups of driving directions with synchronous signaling utilizing 48 pairs of intersection paths. The proposed distance measure which is based on Bayes' model comparison gives the best result. The best accuracy was reached with 93.8 %.

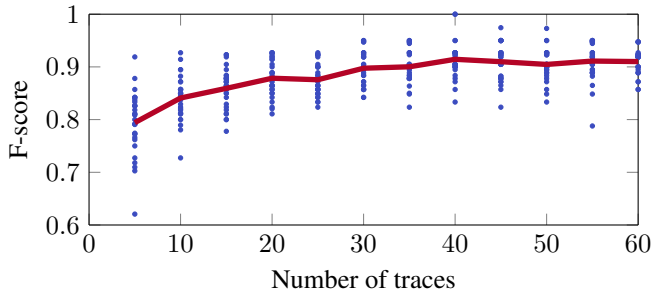

Fig. 11. F-score dependent on the number of traces. The data base contains 32 pairs of intersection paths with at least 60 traces. The evaluated number of traces is sampled randomly from these traces, 30 times respectively. The blue dots represent single results whereas the red curve shows the trend of the mean value of the F-scores.

Characteristic (ROC) Curve [32] is produced which allows the comparison of the different distance measures. Figure 10 shows the resulting ROC curve for the real test data set. The result indicates that the proposed distance measure based on the Bayesian model comparison performs best under the investigated measures. The best possible accuracy of the linear binary classifier is reached at 93.8 % with a corresponding F-score of 0.951. The best accuracy point is marked in Figure 10.

Figure 11 shows the F-score dependent on the number of traces which were used for the evaluation. Out of the 48 pairs of intersection paths with enough traces, there are 32 pairs with at least one path with 60 traces. For every path we select different numbers of traces randomly, 30 times respectively. Afterwards the proposed method to determine the signal grouping of different driving directions is applied. The red curve in Figure 11 shows the trend of the mean resulting F-score dependent on the number of traces used as input for the method. The curve indicates that there is no essential improvement with more than about 40 traces. Altogether the F-scores are worse compared to the results from testing all 48 pairs of paths. The reason is that this analysis is performed on intersections with many traces. These intersections tend to be bigger and more complex thus the signaling varies more compared to intersections with less traces.

B. Improvements on Traffic Light Detection

The previous parts of this work were concerned with methods to automatically extract groups of driving directions at an intersection entry which are controlled by synchronous traffic light signaling. To outline the usefulness of such information an exemplary application in a driver assitance system is discussed below. According to the introduction the information about signal groups has the potential to improve camera based detection of the relevant traffic light signal. Given the scenario in Figure 1 and assuming that the system knows the driver's intention to cross the intersection straight, there are the two options for the signal pattern shwon in the Figure. Utilizing the methods presented in this paper the information that the signals for going straight and turning right are synchronous however the signalling for going left differs. With this information the system is able to infer that only option 1 in Figure 1 is plausible which means that green is the relevant signal.

In this part we evaluate the utilization of automatically generated map information in comparison to a basic approach where the relevant signal is chosen based on the minimal orthogonal distance to the current driving tube. The driving tube is simply derived from the steering wheel angle and every traffic light signal is projected orthogonally onto this circular tube. For the map based approach, a digital map containing the relevant information was automatically built for all tested intersections utilizing the methods introduced in this work. The digital map contains

- positions of intersection centers,
- path information with entry and exit orientation,
- stopline positions and orientations assigned to paths
- and signal group information for paths.

For the evaluation we use a test vehicle with a camera for traffic light detection, GPS and inertial sensors. 344 traces from 38 intersections were collected which correspond to 117 minutes of driving time with at least one observed traffic light signal by the camera system. We evaluate single scenes in a framework with 100 ms cycle time, which results in 70 176 scenes. The outputs of the algorithms are compared to a manually labeled ground truth based on video data. The driver turning intention is a necessary input for the proposed method. We assume that the intention is known, so the turning direction was identified through post processing the position data.

Table II shows the results for the comparison of the map based approach and the simple approach under different testing conditions. One general condition is that 500 ms after a signal change were not considered as the camera system has a detection latency. The results demonstrate an improvement through additional map information of at least 1.5 % over all testing conditions and 2.9 % on average. The closer the vehicle is to the stop line, the smaller is the difference between the approaches. The reason is that the driving tube estimation is more accurate at closer distances which makes the detection of the relevant light easier. Besides the distance, the map based approach also performs better when there are more signal groups for the different driving directions. At intersection entries with one signal group, the detection systems still benefits from map information through a longitudinal distance filter.

TABLE II
EVALUATION OF TH ACCURACY OF A CAMERA BASED TRAFFIC LIGHT DETECTION UNDER DIFFERENT TEST CONDITIONS

Test condition	Accuracy - without map	Accuracy - with map	Number of scenes
$d_S > 0\,m$	95.94 %	98.23 %	67482
$0\,m < d_S < 100\,m$	96.89 %	99.03 %	60754
$d_S > 100\,m$	87.72 %	91.26 %	6728
$75\,m < d_S < 100\,m$	92.96 %	97.72 %	7704
$50\,m < d_S < 75\,m$	97.55 %	99.39 %	9275
$25\,m < d_S < 50\,m$	97.33 %	99.33 %	12645
$0\,m < d_S < 25\,m$	97.62 %	99.16 %	31130
One signal group $0\,m < d_S < 100\,m$	97.47 %	99.75 %	9236
More signal groups $0\,m < d_S < 100\,m$	96.78 %	98.90 %	51518
More signal groups $50\,m < d_S < 100\,m$	94.92 %	98.54 %	15243
More signal groups $75\,m < d_S < 100\,m$	92.61 %	97.79 %	7060

By generating a country-specific statistic over the distance of traffic lights to the stop line, it is possible to avoid false detections from pedestrian lights or another close intersection.

The maximum benefit of the map information results with $4.8\,\%$ at large distances $d_S > 100\,m$ and with $5.2\,\%$ at $75\,m < d_S < 100\,m$ and more signal groups. All of the results are statistically significant, since the sample size is very large with at least 6728 single scenes. A chi-squared test with $\alpha = 0.1\,\%$ was utilized as significance test.

VIII. CONCLUSION

In this work we proposed methods to automatically extract information about intersections with traffic lights from car fleet data. The main contribution of this work is the extraction of groups of driving directions with synchronous traffic light signaling at intersections. To this end a new distance measure on probability distributions is introduced based on a Bayesian model comparison approach. The approach considers the number of available traces and observations in order to get a probability for two driving directions to have synchronous signaling. Basis for the introduced methods is a generic representation of the topology and geometry of an intersection which is also introduced in this work, as well as methods to automatically generate the representation. The evaluation on a real test data set with traces from 48 intersections shows that we achieve $93.8\,\%$ accuracy for the classification of two driving directions to have synchronous signaling.

Furthermore we showed that detecting the releant signal with a camera based traffic light detection system is significantly improved by utilizing the generated map information. Especially at large distances to the stop line of more than $75\,m$ and at traffic lights with more signal groups we achieve improvements in the accuracy of more than $5\,\%$. For highly automated driving in urban areas, a correct decision for stopping or driving at traffic light signals is required at about $75\,m$ before the stop line. Approaching a red light with $60\,km/h$ for example with a desired comfortable deceleration of $1.5\,m/s^2$ on average requires a reliable detection at a distance of $92.6\,m$. These investigations indicate a high potential of automatic map creation and update. Depending on reliability requirements it might still be necessary to manually check the results.

A suggestion for future work is to detect changes of the signal program to further improve the classification of synchronous signaling. Changes of the cycle duration during a day could be detected through finding multiple significant minima of the circular variance. Based on that information and with the distribution of green signals we plan to train a Hidden Markov Model in order to get the signal timing information.

REFERENCES

[1] J. Ziegler, P. Bender, M. Schreiber, H. Lategahn, T. Strauss, C. Stiller, U. Franke, N. Appenrodt, C. G. Keller, E. Kaus, R. G. Herrtwich, C. Rabe, D. Pfeiffer, F. Lindner, F. Stein, F. Erbs, M. Enzweiler, C. Knoppel, J. Hipp, M. Haueis, M. Trepte, C. Brenk, A. Tamke, M. Ghanaat, M. Braun, A. Joos, H. Fritz, H. Mock, M. Hein, and E. Zeeb, "Making Bertha Drive - An Autonomous Journey on a Historic Route," *IEEE Intelligent Transportation Systems Magazine (ITSM)*, vol. 6, no. 2, pp. 8–20, Jan. 2014.

[2] C. Ruhhammer, N. Hirsenkorn, F. Klanner, and C. Stiller, "Crowd-sourced intersection parameters: A generic approach for extraction and confidence estimation," in *IEEE Intelligent Vehicles Symposium (IV)*. IEEE, Jun. 2014, pp. 581–587.

[3] R. de Charette and F. Nashashibi, "Real time visual traffic lights recognition based on Spot Light Detection and adaptive traffic lights templates," in *IEEE Intelligent Vehicles Symposium (IV)*. IEEE, Jun. 2009, pp. 358–363.

[4] D. Nienhuser, M. Drescher, and J. M. Zollner, "Visual state estimation of traffic lights using hidden Markov models," in *IEEE Intelligent Transportation Systems Conference (ITSC)*. IEEE, Sep. 2010, pp. 1705–1710.

[5] J. Levinson, J. Askeland, J. Dolson, and S. Thrun, "Traffic light mapping, localization, and state detection for autonomous vehicles," in *IEEE International Conference on Robotics and Automation (ICRA)*. IEEE, May 2011, pp. 5784–5791.

[6] M. Diaz-Cabrera, P. Cerri, and J. Sanchez-Medina, "Suspended traffic lights detection and distance estimation using color features," in *IEEE Intelligent Transportation Systems Conference (ITSC)*. IEEE, Sep. 2012, pp. 1315–1320.

[7] C. K. H. Wilson, S. Rogers, and S. Weisenburger, "The Potential of Precision Maps in Intelligent Vehicles," in *IEEE International Conference on Intelligent Vehicles*, IEEE, Ed., 1998, pp. 419 –422.

[8] S. Rogers, "Creating and Evaluating Highly Accurate Maps with Probe Vehicles," in *IEEE Intelligent Transportation Systems Conference (ITSC)*. Dearborn, MI, USA: IEEE, 2000, pp. 125–130.

[9] W. Shi, S. Shen, and Y. Liu, "Automatic generation of road network map from massive GPS, vehicle trajectories," in *IEEE Intelligent Transportation Systems Conference (ITSC)*. IEEE, Oct. 2009, pp. 1–6.

[10] R. Carisi, E. Giordano, G. Pau, and M. Gerla, "Enhancing in vehicle digital maps via GPS crowdsourcing," in *IEEE International Conference on Wireless On-Demand Network Systems and Services (WONS)*. Bardonecchia, Italy: IEEE, Jan. 2011, pp. 27–34.

[11] S. Hu, L. Su, H. Liu, H. Wang, and T. Abdelzaher, "Smart Road: A Crowd-Sourced Traffic Regulator Detection and Identification System," in *International Conference on Information processing in sensor networks (IPSN)*. New York, NY, USA: ACM Press, Apr. 2013.

[12] H. Aly, A. Basalamah, and M. Youssef, "Map++: A crowd-sensing system for automatic map semantics identification," in *2014 Eleventh Annual IEEE International Conference on Sensing, Communication, and Networking (SECON)*. IEEE, Jun. 2014, pp. 546–554.

[13] M. M. Haklay and P. Weber, "OpenStreetMap: User-Generated Street Maps," *IEEE Pervasive Computing*, vol. 7, no. 4, pp. 12–18, Oct. 2008.

[14] S. Gehrig, S. Wagner, and U. Franke, "System architecture for an intersection assistant fusing image, map, and GPS information," in *IEEE Intelligent Vehicles Symposium (IV)*. IEEE, 2003, pp. 144–149.

[15] N. Fairfield and C. Urmson, "Traffic light mapping and detection," in *IEEE International Conference on Robotics and Automation (ICRA)*. IEEE, May 2011, pp. 5421–5426.

[16] X. X. Martin Ester, Hans-Peter Kriegel, Jörg S, "A density-based algorithm for discovering clusters in large spatial databases with noise," in *International Conference on Knowledge Discovery and Data Mining (KDD)*. Portland, Oregon, USA: AAAI Press, 1996, pp. 226–231.

[17] K. Fukunaga and L. Hostetler, "The estimation of the gradient of a density function, with applications in pattern recognition," *IEEE Transactions on Information Theory*, vol. 21, no. 1, pp. 32–40, 1975.
[18] RiLSA, "Richtlinien für Lichtsignalanlagen - Lichtzeichenanlagen für den Straßenverkehr," Forschungsgesellschaft für Straßen- und Verkehrswesen e.V, Tech. Rep., 2010.
[19] R. Akcelik and M. Besley, "Queue Discharge Flow and Speed Models for Signalised Intersections," in *The 15th International Symposium on Transportation and Traffic Theory (ISTTT)*, 2002, pp. 99–118.
[20] G. Hoffmann and S.-M. Nielsen, *Beschreibung von Verkehrsabläufen an signalisierten Knotenpunkten*. Bundesministerium für Verkehr, Abt. Straßenbau, 1994.
[21] M. Kerper, C. Wewetzer, A. Sasse, and M. Mauve, "Learning Traffic Light Phase Schedules from Velocity Profiles in the Cloud," in *IEEE International Conference on New Technologies, Mobility and Security (NTMS)*. Istanbul, Turkey: IEEE, May 2012, pp. 1–5.
[22] V. Protschky, S. Feit, and C. Linnhoff-Popien, "On the Potential of Floating Car Data for Traffic Light Signal Reconstruction," in *IEEE Vehicular Technology Conference (VTC Spring)*. IEEE, May 2015.
[23] V. Protschky, C. Ruhhammer, and S. Feit, "Learning Traffic Light Parameters with Floating Car Data," in *IEEE Intelligent Transportation Systems Conference (ITSC)*. IEEE, Sep. 2015, pp. 2438–2443.
[24] K. V. Mardia and P. E. Jupp, *Directional Statistics*. John Wiley & Sons, Inc., 1999.
[25] B. Ajne, "A simple test for uniformity of a circular distribution," *Biometrika*, vol. 55, no. 2, pp. 343–354, Jul. 1968.
[26] D. Krajzewicz, J. Erdmann, M. Behrisch, and L. Bieker, "Recent Development and Applications of SUMO - Simulation of Urban MObility," *International Journal On Advances in Systems and Measurements*, vol. 5, no. 3&4, pp. 128–138, 2012.
[27] S. Kullback and R. A. Leibler, "On Information and Sufficiency," *The Annals of Mathematical Statistics*, vol. 22, no. 1, pp. 79–86, Mar. 1951.
[28] Y. Rubner, C. Tomasi, and L. J. Guibas, "The Earth Mover's Distance as a Metric for Image Retrieval," *International Journal of Computer Vision*, vol. 40, no. 2, pp. 99–121, Nov. 2000.
[29] J. K. Kruschke, *Doing Bayesian Data Analysis: A Tutorial with R and BUGS*. Academic Press, 2010, vol. 1.
[30] A. Gelman, J. B. Carlin, H. S. Stern, D. B. Dunson, A. Vehtari, and D. B. Rubin, *Bayesian Data Analysis*. CRC Press, 2013, vol. 3.
[31] R. E. Kass and A. E. Raftery, "Bayes Factors," *Journal of the american statistical association*, vol. 90, no. 430, pp. 773–795, 1995.
[32] T. Fawcett, "ROC Graphs: Notes and Practical Considerations for Researchers," HP Laboratories, Palo Alto, CA, USA, Tech. Rep., 2003.

Christian Ruhhammer received the Dipl.-Ing. (FH) degree with distinction in electrical engineering from University of Applied Sciences Regensburg in 2010 and the M.Sc. degree in automotive software engineering from Technical University Munich, Germany, in 2012. He is currently working towards his Ph.D. degree at BMW Group in collaboration with Karlsruhe Institute of Technology, Karlsruhe, Germany. His research focuses on the automatic generation of map information from car fleet data through applied statistics and machine learning for the support of driver assistance systems and highly automated driving.

Michael Baumann received his B.Sc. and M.Sc. in Electrical Engineering from the University of Applied Sciences and the Technical University Munich in 2012 and 2015 respectively. He has been a research assistant at BMW Group from 2009-2014. Among others, he has contributed to the work that has been awarded as Best Paper at the IEEE Intelligent Vehicles Conference (IV) 2012. Right now he is working as a test engineer in powertrain development.

Valentin Protschky received his B.Sc. and M.Sc. in Computer Science from the Ludwig-Maximilians-Universität München in 2010 and 2012. He works as a Traffic Technology and Traffic Management Specialist at BMW Group in Munich, Germany. His fields of work includes route planning, vehicle trajectory analysis, knowledge discovery and crowdsourced data mining from big data. During his work at BMW, he set up, among other, a back-end traffic light forecast framework. He is currently a Ph.D. candidate in Computer Science at the Ludwig-Maximilians-Universität München, Germany.

Horst Kloeden received the Dipl.-Ing. degree in Electrical Engineering from Chemnitz University of Technology in 2010 and the M.Sc. degree from the Ohio State University in 2009. From 2010 to 2014 he pursued his Ph.D. degree at the Technical University Munich focusing on pedestrian protection systems. Since 2012, Dr. Kloeden is a project leader at BMW. His fields of work include environment perception sensors, computer vision and machine learning algorithms. Dr. Kloeden received a scholarship from the German National Academic Foundation (2006-2010) and from the Fulbright Commission (2008-2009), respectively. His research work has been awarded with the University Prize of Chemnitz University of Technology in 2010 and the Joseph-Ströbl-Prize in 2014.

Felix Klanner joined BMW in 2007. He was appointed the Director of Future Mobility Research, Singapore, in 2014 as a part of a joint initiative of BMW Group and Nanyang Technological University (NTU), Singapore. Dr. Klanner is a Visiting Associate Professor at NTU and has been lecturing on the driver assistance systems course at the University of Technology in Munich, Germany, since 2008. He has published more than 70 patents in the fields of image processing, driver assistance systems and highly automated driving. Dr. Felix Klanner received his doctoral degree in mechanical engineering from the University of Technology in Darmstadt, Germany. He was awarded his diploma in mechanical engineering by the University of Technology in Munich, Germany.

Christoph Stiller (S'93-M'95-SM'99) studied electrical engineering in Aachen, Germany, and Trondheim, Norway, and received the Diploma and Dr.-Ing. degrees from Aachen University of Technology, Aachen, in 1988 and 1994, respectively. In 1994, he was a Postdoctoral Scientist with INRS Telecommunications, Montreal, Canada. In 1995 he joined the Corporate Research and Advanced Development of Robert Bosch GmbH, Hildesheim, Germany, where he was responsible for computer vision for automotive applications. In 2001 he became full Professor and the Director of the Institute for Measurement and Control Systems with Karlsruhe Institute of Technology, Karlsruhe, Germany. In 2010 he was appointed as a Distinguished Visiting Scientist for three months at the Commonwealth Scientific and Industrial Research Organization, Brisbane, Australia. In 2015 he was guest scientist for 5 months at Bosch RTC and Stanford University in Palo Alto, USA.

Dr. Stiller was the President of the IEEE Intelligent Transportation Systems (ITS) Society (2012-2013) and the Vice President for Publications (2009-2010) and for Member Activities (2006-2008). He has been an Associate Editor of IEEE TRANSACTIONS ON IMAGE PROCESSING (1999-2003), IEEE TRANSACTIONS ON INTELLIGENT TRANSPORTATION SYSTEMS (2004-ongoing) and Senior Editor of the IEEE TRANSACTIONS ON INTELLIGENT VEHICLES (2015-ongoing). He was the Editor-in-Chief of the IEEE ITS Magazine (2009-2011). His Autonomous Vehicle AnnieWAY was a finalist in the Urban Challenge 2007 in the U.S. and the winner of the Grand Cooperative Driving Challenge 2011 in the Netherlands. In 2013 he collaborated with Daimler on the automated Bertha Benz Memorial Tour.